Optimum performance analysis of a two-stage irreversible magnetization Brayton refrigeration system

2006 J. Phys. D: Appl. Phys. 39 4293

(http://iopscience.iop.org/0022-3727/39/20/001)

INSTITUTE OF PHYSICS PUBLISHING JOURNAL OF PHYSICS D: APPLIED PHYSICS

J. Phys. D: Appl. Phys. **39** (2006) 4293–4298 doi:10.1088/0022-3727/39/20/001

Optimum performance analysis of a two-stage irreversible magnetization Brayton refrigeration system

Yue Zhang[1,2], **Bihong Lin**[1,2,3] **and Jincan Chen**[1,2]

[1] CCAST (World Laboratory), PO Box 8730, Beijing 100080, People's Republic of China
[2] Department of Physics, Xiamen University, Xiamen 361005, People's Republic of China
[3] Department of Physics, Quanzhou Normal College, Quanzhou 362000, People's Republic of China

E-mail: jcchen@xmu.edu.cn

Received 7 June 2006, in final form 28 July 2006
Published 29 September 2006
Online at stacks.iop.org/JPhysD/39/4293

Abstract

A two-stage magnetization Brayton refrigeration cycle model using a paramagnetic material as the working substance is established, in which the regeneration and the irreversibility in the adiabatic processes are taken into account. On the basis of the thermodynamic properties of a paramagnetic material, the expressions of some important parameters such as the coefficient of performance, refrigeration load and work input are derived and used to analyse the performance characteristics of the refrigeration cycle. The influence of the inter-magnetization process, irreversibility in the adiabatic processes and regeneration on the performance of the cycle is discussed in detail. The advantage of adding the inter-magnetization process is expounded and the magnetic field ratio related to the inter-magnetization process is optimized. Moreover, the optimal values of the temperatures of the working substance at different state points and the optimally operating region of the cycle are determined. The results obtained here are compared with those derived from some relevant magnetic Brayton refrigeration cycles, and consequently, some significant conclusions are obtained.

1. Introduction

Among new refrigeration technologies, magnetic refrigeration, based on the magnetocaloric effect (MCE), is an environmentally-safe refrigeration technology. It does not have ozone-depleting and greenhouse effects for employing magnetic materials as a refrigerant. The magnetic refrigeration devices can be compact, quite stable and durable compared with traditional vapour compression refrigerators. What is more, magnetic refrigeration is highly efficient. Its efficiency can be 30–60% of the Carnot cycle [1], whereas the efficiency of a vapour compression refrigerator is only 5–10% of the Carnot cycle. Therefore, magnetic refrigeration shows great applicable prospects and has been used in gas liquefaction systems [2] and cryogenic applications [3]. It is also a candidate for room temperature refrigeration [4–8].

Paramagnetic or ferromagnetic materials experience an exothermic change and an entropy decrease when a magnetic field is applied isothermally. This MCE, which is intrinsic to all magnetic materials, is the key to magnetic refrigeration. It is well known that the maximum change in entropy occurs in the vicinity of the Curie temperature. With the development of new materials, magnetic materials with different Curie temperatures for different temperature ranges have been discovered [9–14]. Alloys are perceived to be a solution to the magnetic refrigerant materials with giant MCE, easy preparation and low price [10, 11]. For example, recently, Ames Laboratory researchers Pecharsky and Gschneidner have found that the alloys of gadolinium, silicon and germanium show a big MCE, and by adjusting an alloy's composition one can control the temperature at which the effect is greatest, from near room temperature down to about 30 K [10].

Besides the acquirement of appropriate refrigerants, the optimal design of a refrigerator is another significant problem. Among magnetic refrigeration devices, the active magnetic regenerator (AMR) is a device that can be used to

produce efficient and compact cooling over a broad range of temperatures and has become the main research direction of room temperature refrigeration [5, 6]. An AMR is generally a porous bed of magnetic refrigerant material, which acts as both the refrigerant (coolant) that produces refrigeration and the heat storage medium for the heat transfer fluid. There is not a single cycle describing the thermodynamic process undergone by all the working material, and each section of the AMR experiences a unique cycle which may be similar to some traditional gas processes [5]. Then, the cycles of each section are coupled irreversibly. The system also suffers irreversibility that arises from the bounded area and axial conduction loss [8]. The performance analysis of an AMR using a T–S diagram is impossible. On the other hand, many AMR devices have mimicked a magnetic Brayton cycle in each section of the regenerator bed using four distinct steps in a cycle [1, 5]. Compared with other magnetic refrigeration cycles [15–23], the magnetic Brayton refrigeration cycle [21, 23] has distinct merits—it can employ a regenerator to achieve a large temperature span and is easily operated in room temperature magnetic refrigeration [1, 5, 6]. Thus, it is useful to examine the process to gain a basic understanding by using a single Brayton cycle, and it is quite necessary to further optimize the structure of an irreversible magnetic Brayton cycle.

In the present paper, the irreversible cycle model of a two-stage magnetizable regenerative Brayton refrigeration system working with a magnetic material obeying Curie's law is established. The influence of the inter-magnetization process, irreversibility in the adiabatic processes and regeneration on the performance of the refrigeration cycle is discussed. Moreover, the optimal values of the magnetic field intensity of the inter-magnetization process and the temperatures of the magnetic working substance at different state points are determined. The optimum performance characteristics of the magnetic Brayton refrigeration cycle are revealed.

2. Thermodynamic properties of paramagnetic materials

According to statistics mechanics, the magnetization, entropy and internal energy of a simple paramagnetic salt system can be, respectively, expressed as [24]

$$M = Ng\mu_B J B_J(x), \tag{1}$$

$$S = Nk\left[\ln\sinh\left(\frac{2J+1}{2J}x\right) - \ln\sinh\left(\frac{1}{2J}x\right) - xB_J(x)\right], \tag{2}$$

and

$$U = -NkTxB_J(x) = -\mu_0 HM, \tag{3}$$

where $x = g\mu_0\mu_B JH\beta$, μ_B is the Bohr magneton, μ_0 is the permeability of vacuum, g is Lande's factor, J is the quantum number of angular momentum, H is the magnetic field intensity, N is the number of magnetic moments, k is the Boltzmann constant, $\beta = 1/(kT)$ and $B_J(x) = ((2J+1)/2J)\coth(((2J+1)/2J)x) - (1/2J)\coth((1/2J)x)$ is the Brillouin function.

The entropy described by equation (2) is the entropy caused by magnetic moment. Although the entropy of the magnetic material is mainly composed of two factors, magnetic entropy and lattice entropy, the entropy caused by lattice can often be neglected for paramagnetic materials. In particular, for some materials with a high Debye temperature, the lattice entropy is small in the higher temperature ranges [5]. Even if the lattice entropy is dominant and cannot be neglected, the novel refrigerant in AMR can store the heat generated by lattice and return it to the lattice again when it so needs [4]. Thus, the influence of the lattice entropy has not been considered in this paper.

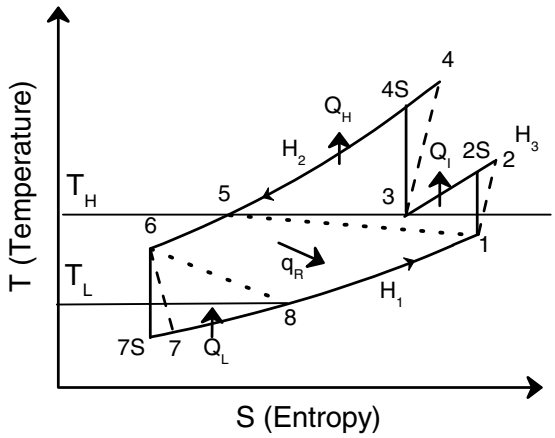

Figure 1. The temperature–entropy (T–S) diagram of a two-stage magnetization Brayton refrigeration cycle system.

When $x \ll 1$, equation (1) becomes the Curie law [25,26], i.e.

$$M = \frac{J(J+1)N\mu_0 g^2\mu_B^2}{3k}\frac{H}{T} = C\frac{H}{T}, \tag{4}$$

where $C = N\mu_0 g^2\mu_B^2 J(J+1)/3k$ is the Curie constant. In this case, the entropy, internal energy and heat capacity at isomagnetic field intensity can be, respectively, derived as

$$S = Nk\ln(2J+1) - \frac{\mu_0 CH^2}{2T^2}, \tag{5}$$

$$U = -\frac{\mu_0 CH^2}{T}, \tag{6}$$

and

$$C_H = T\left(\frac{\partial S}{\partial T}\right)_H = \frac{\mu_0 CH^2}{T^2}. \tag{7}$$

Comprehensive experimental studies have shown that the Curie law is quite accurate for many paramagnetic salts when the temperature goes down to about 1 K, and is even suitable for some paramagnetic salts, such as cerium magnesium nitrate, when the temperature reaches 0.01 K [27]. Thus, the above thermodynamic properties derived from the Curie law can describe the performance of the paramagnetic and ferromagnetic materials when their temperature is over the Curie temperature. This implies that the thermodynamic properties of paramagnetic materials derived from the Curie law is of general significance for discussion in the present paper.

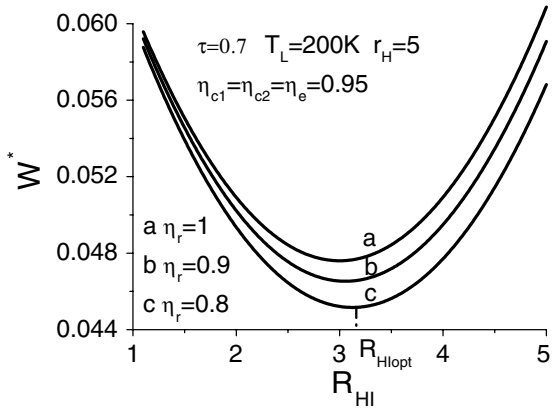

Figure 2. The $W^* \sim R_{HI}$ curves, where $W^* = W/(\mu_0 C H_1^2)$ and the parameters $\tau = 0.7$, $T_L = 200\,\mathrm{K}$, $\eta_{c1} = \eta_{c2} = \eta_e = 0.95$ and $r_\mathrm{H} = 5$ are chosen.

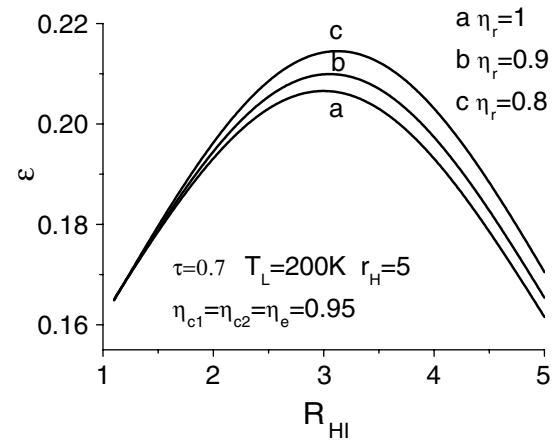

Figure 3. The $\varepsilon \sim R_{HI}$ curves, where the parameters are the same as those used in figure 2.

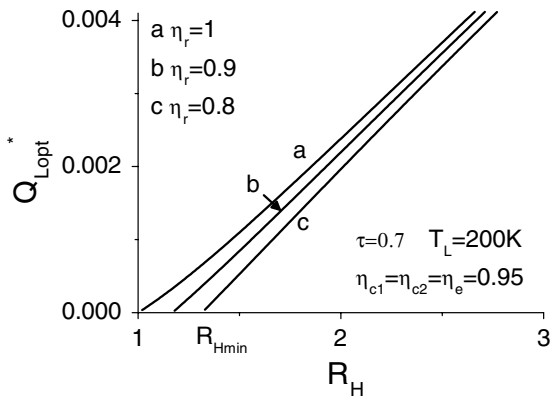

Figure 4. The $Q^*_{L\mathrm{opt}} \sim r_\mathrm{H}$ curves, where $Q^*_{L\mathrm{opt}} = Q_{L\mathrm{opt}}/(\mu_0 C H_1^2)$ and the parameters $\tau = 0.7$, $T_L = 200\,\mathrm{K}$ and $\eta_{c1} = \eta_{c2} = \eta_e = 0.95$ are chosen.

3. An irreversible cycle model

Figure 1 shows the temperature–entropy diagram of a two-stage magnetizable regenerative Brayton magnetic refrigeration cycle using a paramagnetic material as the working substance. The structure of this model is similar to the multi-compression gas refrigerator which has been widely

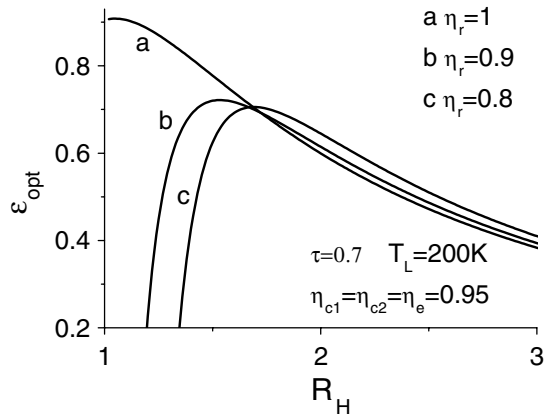

Figure 5. The $\varepsilon_\mathrm{opt} \sim R_H$ curves, where the parameters are the same as those used in figure 4.

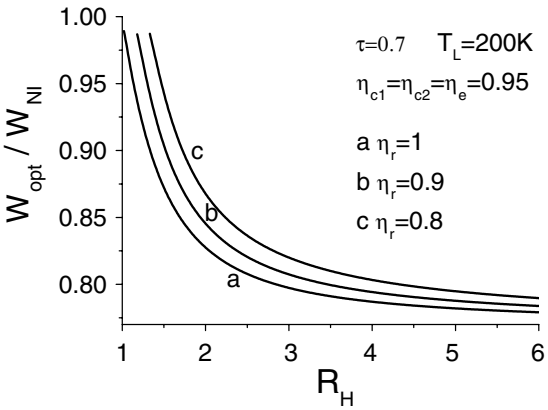

Figure 6. The $W_\mathrm{opt}/W_{NI} \sim R_H$ curves, where the parameters are the same as those used in figure 4.

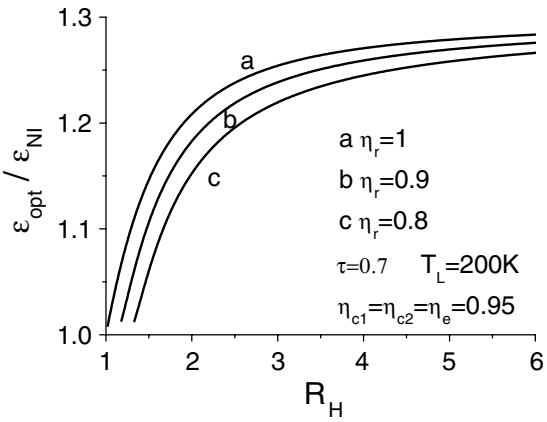

Figure 7. The $\varepsilon_\mathrm{opt}/\varepsilon_{NI} \sim R_H$ curves, where the parameters are the same as those used in figure 4.

used in practical fields [28]. In figure 1, 7–8, 4–5 and 2–3 are, respectively, the three heat exchange processes with the constant magnetic field intensities H_1, H_2 and H_3, 6–7S, 1–2S and 3–4S are the three reversible adiabatic processes while 6–7, 1–2 and 3–4 are the three irreversible adiabatic processes. The regeneration is carried out during the two heat exchange processes 5–6 and 8–1; Q_R is the amount of regeneration and Q_L, Q_H and Q_I are, respectively, the amounts of heat

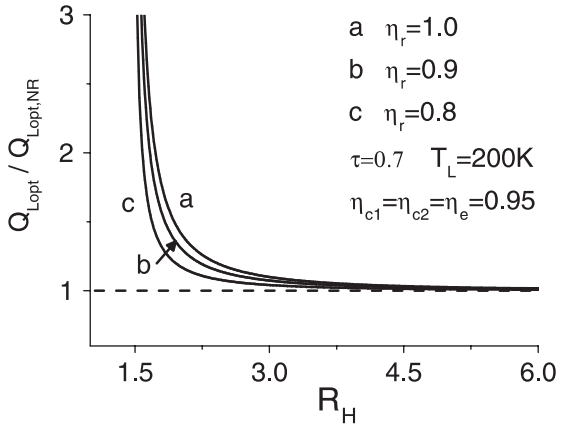

Figure 8. The $Q^*_{Lopt}/Q_{Lopt,NR} \sim R_H$ curves, where the parameters are the same as those used in figure 4.

exchange between the working substance in the three constant magnetic field processes and the heat reservoirs. T_H and T_L are the temperatures of the high- and low-temperature reservoirs and the temperatures of the working substance at the state points 1, 2, 3, 4, 5, 6, 7 and 8 are represented by T_1, T_2, T_H, T_4, T_H, T_6, T_7 and T_L, respectively.

For the three reversible adiabatic processes, one can find the following relations

$$\frac{T_6}{T_{7S}} = \frac{H_2}{H_1} = R_H, \qquad \frac{T_{2S}}{T_1} = \frac{H_3}{H_1} = R_{HI},$$
$$\frac{T_{4S}}{T_3} = \frac{H_2}{H_3} = R_H R_{HI}^{-1}, \tag{8}$$

from equation (5), where $R_H = H_2/H_1$ is the maximum ratio of the magnetic field intensities and $R_{HI} = H_3/H_1$ is the ratio of the magnetic field intensity of the inter-magnetization process to the minimum magnetic field intensity. When $R_{HI} = 1$ or $R_{HI} = R_H$, the cycle is simplified as a magnetic Brayton refrigeration cycle which consists of two isomagnetic fields and two adiabatic processes.

When the three adiabatic processes are irreversible, one can introduce the expansion and compression efficiencies

$$\eta_e = (T_6 - T_7)/(T_6 - T_{7S}), \tag{9}$$

$$\eta_{c1} = (T_{2S} - T_1)/(T_2 - T_1), \tag{10}$$

and

$$\eta_{c2} = (T_{4S} - T_3)/(T_4 - T_3) \tag{11}$$

to describe the degree of the irreversibility in the three adiabatic processes, respectively.

By using equations (8)–(11), the temperatures of the working substance at the state points 1, 7, 2 and 4 can be expressed as

$$T_1 = \eta_r T_H = \eta_r T_L \tau^{-1}, \tag{12}$$

$$T_7 = X T_6, \tag{13}$$

$$T_2 = Y T_1 = Y \eta_r T_L \tau^{-1}, \tag{14}$$

and

$$T_4 = Z T_H = Z T_L \tau^{-1}, \tag{15}$$

where $X = \eta_e(R_H^{-1} - 1) + 1$, $Y = \eta_{c1}^{-1}(R_{HI} - 1) + 1$, $Z = \eta_{c2}^{-1}(R_H R_{HI}^{-1} - 1) + 1$. $\tau = T_L/T_H$ is the temperature ratio of the two reservoirs and $\eta_r = T_1/T_H$ is the regeneration factor. When $\eta_r = 1$, the cycle is operated with a maximum regeneration; while $\eta_r = \tau$, the cycle is operated without regeneration. Thus, the range of η_r is $\tau \leqslant \eta_r \leqslant 1$. Only when $T_2 > T_H$ can heat be rejected to the high-temperature reservoir during the inter-magnetization process, so there is the following relation,

$$R_{HI} > R_{HI\,\min} = \eta_{c1}(\eta_r^{-1} - 1) + 1. \tag{16}$$

By using equation (7), the regenerative heat can be expressed as

$$Q_R = \mu_0 C H_2^2 (T_6^{-1} - T_H^{-1}) = \mu_0 C H_1^2 (T_L^{-1} - T_1^{-1}). \tag{17}$$

Solving equations (12) and (17) gives

$$T_6 = T_L[R_H^{-2}(1 - \tau\eta_r^{-1}) + \tau]^{-1}. \tag{18}$$

Equations (12)–(15) and (18) indicate that the temperatures T_1, T_2, T_4, T_6 and T_7 can be expressed as the function of T_L, τ, R_H, R_{HI}, η_{c1}, η_{c2}, η_e and η_r.

According to the cycle model shown in figure 1 and by using equations (7) and (13)–(15), the various heat transfers (Q_H, Q_L and Q_I) can be given by

$$Q_H = \mu_0 C H_2^2 (T_H^{-1} - T_4^{-1}) = \mu_0 C H_2^2 T_L^{-1} \tau (1 - Z^{-1}), \tag{19}$$

$$Q_L = \mu_0 C H_1^2 (T_7^{-1} - T_L^{-1})$$
$$= \mu_0 C H_1^2 T_L^{-1} \tau \{X^{-1}[R_H^{-2}(\tau^{-1} - \eta_r^{-1}) + 1] - \tau^{-1}\}, \tag{20}$$

and

$$Q_I = \mu_0 C H_3^2 (T_H^{-1} - T_2^{-1}) = \mu_0 C H_3^2 T_L^{-1} \tau (1 - Y^{-1}\eta_r^{-1}). \tag{21}$$

Flowing through the AMR, the heat transfer fluid carries heat generated by magnetic materials (Q_H, Q_L, Q_R and Q_I) to and from the magnetic refrigerant [5, 6]. In an ideal active magnetic regenerative refrigeration cycle, all heat is transferred instantaneously between the magnetic solid and the heat transfer fluid. Thus, selecting a proper substance with proper heat capacity as heat transfer fluid for keeping the balance of AMR is important in design.

It can be seen from equation (20) that the amount of cooling load is dependent on τ, R_H and η_r, but independent of R_{HI}. The input work and coefficient of performance (COP) of the cycle can be expressed as

$$W = Q_H + Q_I - Q_L$$
$$= \mu_0 C H_1^2 T_L^{-1} \tau \{R_H^2(1 - Z^{-1}) + R_{HI}^2(1 - Y^{-1}\eta_r^{-1})$$
$$- X^{-1}[R_H^{-2}(\tau^{-1} - \eta_r^{-1}) + 1] + \tau^{-1}\} \tag{22}$$

and

$$\varepsilon = \frac{Q_L}{W} = \{X^{-1}[R_H^{-2}(\tau^{-1} - \eta_r^{-1}) + 1] - \tau^{-1}\}$$
$$\{R_{HI}^2(1 - Y^{-1}\eta_r^{-1}) + R_H^2(1 - Z^{-1})$$
$$- X^{-1}[R_H^{-2}(\tau^{-1} - \eta_r^{-1}) + 1] + \tau^{-1}\}^{-1}. \tag{23}$$

4. Performance analysis and parametric optimization

For an assumed value of the total magnetic field ratio, equations (22) and (23) can be used to generate the $W^* \sim R_{HI}$ and $\varepsilon \sim R_{HI}$ curves, as shown in figures 2 and 3, respectively, where $W^* = W/(\mu_0 C H_1^2)$, and the parameters $\tau = 0.7$, $T_L = 200\,\mathrm{K}$, $\eta_{c1} = \eta_{c2} = \eta_e = 0.95$ and $R_H = 5$ are chosen. It is seen from the curves in figures 2 and 3 that there exists an optimal magnetic field ratio ($R_{HI,\mathrm{opt}}$) at which the work input is minimum, while the COP attains its maximum.

With the help of the values of $R_{HI,\mathrm{opt}}$ determined by different R_H, one can generate the $Q^*_{L\mathrm{opt}} \sim R_H$ and $\varepsilon_{\mathrm{opt}} \sim R_H$ curves, as shown in figures 4 and 5, respectively, where $Q^*_{L\mathrm{opt}} = Q_{L\mathrm{opt}}/(\mu_0 C H_1^2)$ and the parameters $\tau = 0.7$, $T_L = 200\,\mathrm{K}$ and $\eta_{c1} = \eta_{c2} = \eta_e = 0.95$ are chosen. The curves in figure 4 show that there exists the minimum value of the total magnetic field ratio ($R_{H\,\mathrm{min}}$). When $\eta_r < 1$, $R_{H\,\mathrm{min}} > 1$. It implies that the cycle must be operated in the range of $R_H > R_{H\,\mathrm{min}}$, otherwise the cooling load is smaller than zero and consequently the refrigeration cycle cannot play a positive role. It can also be seen from figures 4 and 5 that the cooling load is a monotonic increasing function of the total magnetic field ratio, while the COP is not, in general, a monotonic function of the total magnetic field ratio. When $\eta_r < 1$, the COP first increases and then decreases with R_H, so that there is a maximum for the COP. When $\eta_r = 1$, the COP is a monotonic decreasing function of R_H.

With the help of the values of $R_{HI,\mathrm{opt}}$ determined by different R_H, one can also compare the performance of the Brayton refrigeration cycle incorporating an optimal inter-magnetization process with that without the inter-magnetization process. For example, one can generate $W_{\mathrm{opt}}/W_{NI} \sim R_H$ and $\varepsilon_{\mathrm{opt}}/\varepsilon_{NI} \sim R_H$ curves, as shown in figures 6 and 7, respectively, where W_{NI} and ε_{NI} are the work input and COP of a regenerative magnetic Brayton refrigeration cycle without the inter-magnetization process and the parameters are the same as those used in figure 4. It can be clearly seen from figures 6 and 7 that the use of the inter-magnetization process always reduces the work input and consequently increases the COP. The larger the ratio, R_H, of the magnetic field intensities, the more obvious the advantage of adding the inter-magnetization process. Therefore, in practical applications, the inter-magnetization process can be adopted to enhance the performance of magnetic Brayton refrigeration cycles.

It should be noted that when $\eta_r = \tau$, i.e. $T_1 = T_L$, $T_6 = T_H$, the cycle is operated without regeneration. In this case, one can also do similar optimization for the inter-magnetization process. Thus, the optimal performance of the Brayton refrigeration cycle with regeneration can be compared with that without ingeneration. For example, one can generate $Q_{L,\mathrm{opt}}/Q_{L\mathrm{opt},NR} \sim R_H$ and $\varepsilon_{\mathrm{opt}}/\varepsilon_{\mathrm{opt},NR} \sim R_H$ curves, as shown in figures 8 and 9, respectively, where the subscript NR indicates the cycle without the regeneration process and the parameters are the same as those used in figure 4. The curves in figures 8 and 9 show clearly that the incorporation of regeneration will always enhance the cooling load which is significant for a refrigeration cycle. In the Brayton refrigeration cycle with a small total magnetic field ratio, the incorporation of regeneration even enhances the COP. Therefore, regeneration plays an extraordinarily important role in the Brayton refrigeration cycle with a small total magnetic field ratio.

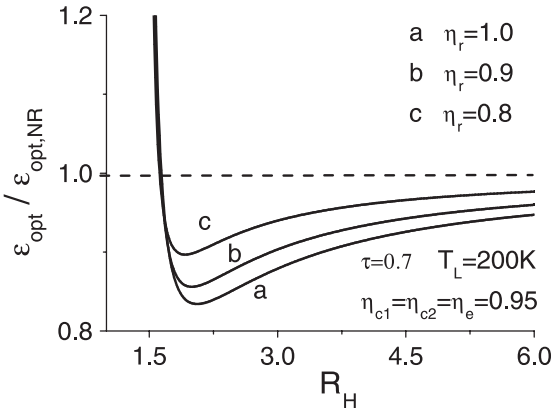

Figure 9. The $\varepsilon_{\mathrm{opt}}/\varepsilon_{\mathrm{opt},NR} \sim R_H$ curves, where the parameters are the same as those used in figure 4.

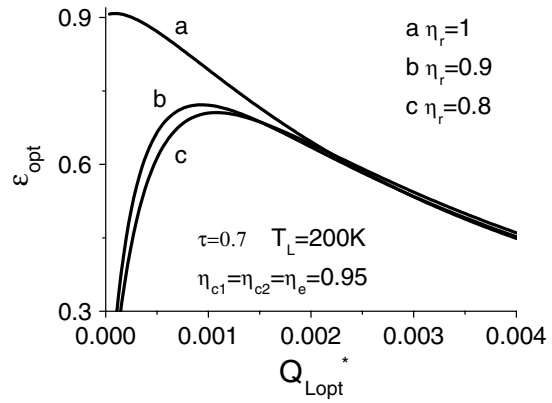

Figure 10. The $\varepsilon_{\mathrm{opt}} \sim Q^*_{L\mathrm{opt}}$ curves, where the parameters are the same as those used in figure 4.

What is more, one can plot the $\varepsilon_{\mathrm{opt}} \sim Q^*_{L\mathrm{opt}}$ curves, as shown in figure 10, where the parameters are the same as those used in figure 4. It can be seen from figure 10 that there exists an optimal working range for a magnetic Brayton refrigeration cycle, i.e. the part of the curve with a negative slope. When the cycle is operated in such a range, the cooling load will increase as the efficiency decreases, and vice versa.

In addition, the maximum COP of the cycle system and its corresponding optimum cycle parameters can be calculated and listed in table 1, where the parameters $\tau = 0.7$ and $T_L = 200\,\mathrm{K}$ are chosen. The data in table 1 show that the irreversibility in the adiabatic process always poses a negative influence on the performance of the refrigeration cycle, i.e. the COP of the cycle system will decrease while the magnetic field intensity ratio and the temperature span of the working substance will increase as the irreversibility in the adiabatic process increases.

5. Conclusions

The irreversible cycle model of a two-stage magnetization Brayton refrigerator working with a paramagnetic material

Table 1. The values of $\varepsilon_{\max}$ and the corresponding parameters, where the parameters $\tau = 0.7$ and $T_L = 200$ K are chosen.

$\eta_{c1} = \eta_{c2} = \eta_e$	η_r	$\varepsilon_{\max}$	$R_{H\,\mathrm{opt}}$	$R_{HI\,\mathrm{opt}}$	$T_{1\mathrm{opt}}$	$T_{2\mathrm{opt}}$	$T_{4\mathrm{opt}}$	$T_{6\mathrm{opt}}$	$T_{7\mathrm{opt}}$
0.95	0.9	0.72	1.53	1.32	257	344	333	251	169
	0.8	0.71	1.69	1.47	229	342	331	269	165
	0.7	0.77	1.77	1.60	200	326	318	285	168
0.90	0.9	0.50	1.60	1.35	257	359	343	254	168
	0.8	0.47	1.79	1.52	228	361	341	270	163
	0.7	0.47	1.93	1.68	200	352	332	285	162
0.85	0.9	0.36	1.67	1.40	257	376	353	256	169
	0.8	0.32	1.89	1.57	228	383	353	272	163
	0.7	0.31	2.06	1.75	200	377	345	286	161

is set up. By using the thermodynamic properties of a paramagnetic material, the expressions of some important parameters such as the COP, refrigeration load and work input are derived and used to reveal the performance characteristics of this cycle. The influence of the inter-magnetization process and regeneration process on the performance of the cycle is analysed in detail. It is found that the adoption of the inter-magnetization process can remarkably enhance the performance of a magnetic Brayton refrigeration cycle, i.e. it will reduce the amount of work input and consequently increase the COP. It is also found that the incorporation of regeneration will always enhance the cooling load, and even enhances the COP when the total magnetic field ratio is small. Moreover, the optimal magnetic field ratios, the optimal values of the working substance temperatures at different state points and the optimally operating region of the cycle are determined. The results obtained will be helpful in the optimal design of the magnetic Brayton refrigeration cycle for the purpose of saving energy and applying new magnetic refrigeration technologies.

Acknowledgments

This work has been supported by the Key Project Foundation of Science and Technology Research of Ministry of Education, People's Republic of China.

References

[1] Zimm C, Jastrab A, Sternberg A, Pecharsky VK, Gschneidner Jr KA, Osborne M and Anderson I 1998 *Adv. Cryog. Eng.* **43** 1759
[2] Zhang L, Sherif S A, DeGregoria A J, Zimm C and Veziroglu T N 2000 *Cryogenics* **40** 269
[3] Shirron P, Canavan E, DiPirro M, Jackson M, King T, Panek J and Tuttle J 2002 *Cryogenics* **41** 789
[4] Reid C E, Barclay J A, Hall J L and Sarangi S 1994 *J. Alloys Compounds* **207** 366
[5] Yu B, Gao Q, Zhang B, Meng X and Chen Z 2003 *Int. J. Refrig.* **26** 622
[6] Pecharsky V K and Gschneidner K A Jr 1999 *J. Magn. Magn. Mater.* **200** 44
[7] Hirano N, Nagaya S, Takahashi M, Kuriyama T, Ito K and Nomura S 2002 *Adv. Cryog. Eng.* **47** 1027
[8] Shir F, Mavriplis C, Bennett L H and Torre E D 2005 *Int. J. Refrig.* **28** 616
[9] Bruck E, Tegus O, Li X W, de Boer F R and Buschow K H J 2003 *Physica* B **327** 431
[10] Pecharsky V K and Gschneidner K A Jr 1997 *Appl. Phys. Lett.* **70** 3299
[11] Provenzano V, Shapiro A J and Shull R D 2004 *Nature* **429** 853
[12] Tegus O, Bruck E, Buschow K H J and de Boer F R 2002 *Nature* **415** 150
[13] Tegus O, Bruck E, Zhang L, Dagula W, Buschow K H J and de Boer F R 2002 *Physica* B **319** 174
[14] Hu F X, Shen B G, Sun J R and Cheng Z H 2001 *Phys. Rev.* B **64** 012409
[15] Lin G, Tegus O, Zhang L and Bruck E 2004 *Physica* B **344** 147
[16] Rowe A M and Barclay J A 2003 *J. Appl. Phys.* **93** 1672
[17] He J, Chen J and Wu C 2003 *J. Energy Res. Technol.* **125** 318
[18] He J, Chen J and Wu C 2002 *J. Non-Equilib. Thermodyn.* **27** 57
[19] Chen J and Yan Z 1998 *J. Appl. Phys.* **84** 1791
[20] Wu F, Chen L, Wu C, Sun F and Zhu Y 2001 *Int. J. Eng. Sci.* **39** 361
[21] Chen L and Yan Z 1994 *J. Appl. Phys.* **73** 1249
[22] Wu C, Chen L and Chen J 1999 *Recent Advances in Finite-Time Thermodynamics* (New York: Nova Science)
[23] Yang Y, Chen J, He J and Bruck E 2005 *Physica* B **364** 33
[24] Pathria R K 1972 *Statistical Mechanics* 2nd edn (Oxford: Pergamon)
[25] Vonsovskii S V 1974 *Magnetism* (New York: Wiley)
[26] Zemansky M W 1968 *Heat and Thermodynamics* 5th edn (New York: McGraw-Hill)
[27] Mandl F 1970 *Statistical Physics* (London: Wiley)
[28] Bard S 1986 *Cryogenics* **26** 450